

FOXO1 Plays an Important Role in Enhanced Microvascular Cell Apoptosis and Microvascular Cell Loss in Type 1 and Type 2 Diabetic Rats

Yugal Behl,¹ Padmaja Krothapalli,¹ Tesfahun Desta,¹ Sayon Roy,² and Dana T. Graves³

OBJECTIVE—To investigate early events leading to microvascular cell loss in diabetic retinopathy.

RESEARCH DESIGN AND METHODS—FOXO1 was tested in vivo by DNA binding activity and by nuclear translocation in microvascular cells in retinal trypsin digests. In vivo studies were undertaken in STZ-induced diabetic rats and Zucker diabetic fatty rats using the tumor necrosis factor (TNF)-specific blocker, pegsunercept, or by inhibiting FOXO1 with RNAi. Microvascular cell apoptosis, formation of pericyte ghosts, and acellular capillaries were measured. Upstream and downstream effects of high-glucose-induced FOXO1 were tested on rat microvascular endothelial cells (RMECs) by small-interfering RNA (siRNA) in vitro.

RESULTS—DNA binding or nuclear translocation of FOXO1, which was reduced by TNF inhibition, was elevated in type 1 and type 2 diabetic retinas. Diabetes stimulated microvascular cell apoptosis; pericyte ghost and acellular capillary development was inhibited by FOXO1 siRNA. High glucose in vitro decreased FOXO1 phosphorylation and DNA binding activity and decreased Akt phosphorylation in RMECs. High-glucose-stimulated FOXO1 DNA binding activity was mediated through TNF- α and formation of reactive oxygen species (ROS), while inhibitors of TNF and ROS and FOXO1 siRNA reduced high-glucose-enhanced RMEC apoptosis. The caspase-3/7 activity and capacity of high glucose to increase mRNA levels of several genes that regulate RMEC activation and apoptosis were knocked down by FOXO1 siRNA.

CONCLUSIONS—FOXO1 plays an important role in rat retinal microvascular cell loss in type 1 and type 2 diabetic rats and can be linked to the effect of high glucose on FOXO1 activation. *Diabetes* 58:917–925, 2009

D iabetic retinopathy, the leading cause of vision loss in occupational-age adults (1,2), is characterized by early vascular lesions, including apoptosis of microvascular cells, formation of pericyte ghosts, and the development of acellular capillaries before the onset of clinical complications (3,4). The formation of acellular capillaries eventually leads to hyp-

oxia, setting the stage for proliferative diabetic retinopathy that ultimately results in impaired vision (5–8).

The loss of critical microvascular cells in the early stages of this complication are not well understood. To investigate this issue, we examined in type 1 and type 2 diabetic rats the role of the transcription factor FOXO1, a forkhead transcription factor that regulates cell death, inhibits cell cycle progression, and modulates differentiation in various cell types (9–11). FOXO1 also has cell-specific effects modulating genes that control gluconeogenesis (12), blood vessel assembly during development (13), muscle wasting (14), and inhibition of adipocyte differentiation (15).

We recently showed that diabetes-induced tumor necrosis factor (TNF)- α plays an important role in microvascular cell loss (16). We demonstrate here for the first time that diabetes enhances FOXO1 DNA binding activity and nuclear translocation in diabetic retinas through a process that is mediated by TNF. Furthermore, inhibition of FOXO1 by RNAi reduces microvascular cell apoptosis and microvascular cell loss in diabetic retinas in vivo and by high glucose in vitro. These results point to the previously unrecognized role of FOXO1 in promoting apoptosis and loss of microvascular cells in diabetic retinopathy.

RESEARCH DESIGN AND METHODS

Type 1 diabetic ~8-week-old Sprague Dawley (SD) rats (Charles River Laboratories, Wilmington, MA) were injected intraperitoneally with streptozotocin (STZ) (55 mg/kg), and control animals received vehicle (0.05 mol/l citrate buffer). Animals were subcutaneously injected with 1–5 units of NPH insulin as needed to maintain serum glucose levels of ~300 mg/dl. Type 2 diabetes was studied in Zucker diabetic fatty rats (*fa/fa*) (ZDF) and genetically matched lean controls (*fa/+*) (Charles River Laboratories). Unless stated, there were 6 animals per group, except for diabetic rats treated with vehicle alone, which consisted of 12 animals per group. Serum glucose and weight were monitored weekly. Glycosylated hemoglobin was measured (Helena Laboratories, Beaumont, TX) when rats were killed. For short-term studies, rats were killed ~12 weeks after the onset of diabetes; for long-term studies, they were hyperglycemic for ~6 months and killed at age 33–34 weeks. All measurements were performed by two blinded examiners.

Application of inhibitors. In short-term studies, FOXO1-specific small-interfering RNA (siRNA) (CCA GCT ATA AAT GCA CAT TTA) or scrambled siRNA (45 pmol in 5 μ l sterile water) was intravitreally injected in diabetic rats that were hyperglycemic for 12 weeks ($n = 5$); they were killed 10 days after injection (17). There is no significant homology between the sequence used for FOXO1 siRNA and other forkhead box proteins. For long-term RNAi in STZ, rats were hyperglycemic for 12 weeks and then given two intravitreal injections of siRNA (45 pmol in 5 μ l sterile water) 6 weeks apart. The ZDF rats received one intravitreal injection after 24 weeks of hyperglycemia and killed 10 days later.

In STZ-induced diabetic rats, pegsunercept (peg-TNFR1; 50 μ g) (Amgen, Thousand Oaks, CA) was applied by intravitreal injections 6, 12, and 18 weeks after becoming hyperglycemic. Pegsunercept was given to ZDF rats 12 and 18 weeks after becoming hyperglycemic. Pegsunercept is a specific TNF inhibitor consisting of a pegylated recombinant soluble TNF receptor-1 (18). For both groups controls received vehicle (sterile PBS) alone.

Apoptosis, acellular capillaries, and pericyte ghosts. Retinal trypsin digests (RTDs) were assessed by a fluorometric terminal dUTP nick-end

From the ¹Department of Periodontology and Oral Biology, Boston University School of Dental Medicine, Boston, Massachusetts; the ²Departments of Medicine and Ophthalmology, Boston University School of Medicine, Boston, Massachusetts; and the ³Department of Periodontics, University of Medicine and Dentistry of New Jersey, Newark, New Jersey.

Corresponding author: Dana T. Graves, gravesdt@umdnj.edu.

Received 22 April 2008 and accepted 16 December 2008.

Published ahead of print at <http://diabetes.diabetesjournals.org> on 23 January 2009. DOI: 10.2337/db08-0537.

© 2009 by the American Diabetes Association. Readers may use this article as long as the work is properly cited, the use is educational and not for profit, and the work is not altered. See <http://creativecommons.org/licenses/by-nc-nd/3.0/> for details.

The costs of publication of this article were defrayed in part by the payment of page charges. This article must therefore be hereby marked "advertisement" in accordance with 18 U.S.C. Section 1734 solely to indicate this fact.

labeling (TUNEL) assay (Promega, San Luis Obispo, CA) and by immunohistochemistry using an antibody specific for activated caspase-3 (Cell Signaling Technology, Danvers, MA). RTDs were permeabilized (0.5% Triton X-100) and incubated with blocking agent (Chemicon, Temecula, CA), primary or matched control antibody, and biotinylated secondary antibody and fluorescein avidin (Vector Laboratories, Burlingame, CA). Mounting media contained nuclear stain 4',6-diamidino-2-phenylindole (DAPI) (Vector Laboratories). The entire specimen was surveyed for TUNEL-positive or caspase-3-positive cells by fluorescence microscopy (original magnification $\times 400$). RTDs were stained with periodic acid Schiff (PAS)-hematoxylin (6), and 13–15 fields in the midretina were examined as described (16).

FOXO1 nuclear translocation. FOXO1 nuclear translocation was detected by confocal laser-scanning microscopy (Axiovert-100M; Carl Zeiss). Primary antibody to FOXO1 (Santa Cruz Biotech, Santa Cruz, CA) was detected by a Cy5-tagged secondary antibody and nuclei with propidium iodide. The entire RTD was scanned for nuclear FOXO1-positive microvascular cells examining single and merged images. Matched control IgG was negative, demonstrating specificity (data not shown).

FOXO1 DNA binding. Nuclear protein from whole retinas of rats that were hyperglycemic for 12 weeks and matched normoglycemic controls was measured using a kit from Pierce Biotechnology (Rockford, IL). FOXO1 DNA binding activity was examined in nuclear extracts with a transcription factor DNA binding kit (Active Motif, Carlsbad, CA).

Real-time PCR. Retinas of STZ-induced diabetic rats, hyperglycemic for 12 weeks with or without pegsunercept for the last 8 weeks, and age-matched control rats ($n = 6$) were snap frozen (16). Total RNA (RNAeasy Mini Kit; Qiagen, Valencia, CA) was isolated and FOXO1 mRNA levels quantified by real-time PCR using TaqMan primers and probes (Applied Biosystems, Foster City, CA).

FOXO1 DNA binding and caspase-3/7 activity in vitro. Rat microvascular endothelial cells (RMECs) were isolated, characterized, and cultured as described (17,19) and examined at passages 3–8. Cells were cultured in DMEM plus 10% fetal bovine serum (FBS) and changed to 0.5% FBS at least 24 h before the start of experiments. In some experiments, RMECs were preincubated with 10 mmol/l *N*-acetyl-L-cysteine (NAC) (Sigma-Aldrich) for 2 h followed by incubation with media supplemented with glucose (25 mmol/l) and NAC as indicated. Nuclear protein was isolated and assayed for FOXO1 DNA binding activity (Active Motif). Cytoplasmic proteins were extracted using a kit from Pierce Biotechnology, and caspase-3/7 activity was measured with a caspase-glo 3/7 kit from Promega (Mannheim, Germany).

FOXO1 and AKT phosphorylation. RMECs were cultured in 96-well plates in DMEM plus 0.25% FBS, transfected with or without rat FOXO1-specific siRNA (5 nmol/l in HiPerfect transfection reagent), or scrambled siRNA (Qiagen) and then incubated in high-glucose media (25 mmol/l) for 5 days. Some wells were incubated with Akt inhibitor (Calbiochem, Gibbstown, NJ). FOXO1 protein, phosphorylated FOXO1, total AKT protein, and phosphorylated AKT levels were determined by using an in situ detection kit from Active Motif. Cells were incubated in high glucose; fixed with 4% paraformaldehyde; permeabilized; and incubated with blocking solution followed by primary antibodies to FOXO1, phosphorylated FOXO1, AKT, phosphorylated AKT, or matched control antibody followed by horseradish peroxidase-conjugated secondary antibody. After addition of colorimetric substrate, optical density was measured at 450 nm and corrected for cell number by crystal violet staining and optical density at 695 nm.

Apoptosis in vitro. RMECs were cultured in DMEM plus 0.25% FBS and transfected with or without rat FOXO1-specific siRNA (5 nmol/l in HiPerfect transfection reagent) or scrambled siRNA (Qiagen) and then incubated with TNF- α (20 ng/ml, 6 h) or media supplemented with glucose or mannitol (25 mmol/l) for 5 days. Some RMECs were incubated with 10 mmol/l of NAC (Sigma-Aldrich) or the caspase-3/7-specific inhibitor (Z-DEVD-FMK; R&D Systems) plus high glucose (25 mmol/l) for 5 days. Apoptosis was measured by enzyme-linked immunosorbent assay (ELISA) measuring cytoplasmic histone-associated DNA (Roche Diagnostics), as we have described (20).

Focused microarray analysis and real-time PCR validation. Total RNA was isolated (RNAeasy; Qiagen) from primary RMECs transfected with FOXO1 or scrambled siRNA, as described above, and then incubated in standard media or media supplemented with glucose or mannitol (25 mmol/l) for 5 days. Focused microarrays (Oligo GEArray; SuperArray, Bethesda, MD) were carried out as we have described (21), and the spot intensity from chemiluminescent images were analyzed using the GeaSuite array analysis (SuperArray). Spot intensities were normalized with ribosomal protein (L32). A value was considered to be modulated if both the mean and the median intensity level in the experimental group was 1.7-fold higher or lower than that of the mean of the corresponding control. Selected genes were confirmed by real-time PCR (Applied Biosystems). Assays were carried out three times to provide means \pm SE.

Statistical analysis. For all in vitro assays, experiments were carried out three times to provide means \pm SE. Statistical significance was determined by one-way ANOVA with Tukey's post hoc test for comparisons between multiple groups at the $P < 0.05$ level.

RESULTS

Type 1 diabetic rats had reduced weight and higher glycosylated hemoglobin levels compared with normoglycemic rats, while type 2 diabetic rats weighed more and had higher glycosylated hemoglobin levels compared with normoglycemic littermates (data not shown). Treatment with siRNA or pegsunercept had no effect on these parameters (data not shown).

Diabetes increased FOXO1 nuclear translocation in microvascular cells in vivo and mediated by TNF- α .

FOXO1 nuclear translocation was examined in retinal trypsin digests (RTDs) containing isolated microvascular cells by laser-scanning confocal microscopy. It reflects the activation status since FOXO1 is rapidly transported to the nuclear compartment in the activated state and upon deactivation is quickly transported out of the nucleus (10,11). Confocal microscopy avoids some of the pitfalls of standard immunofluorescence since the images are taken at a focal plane that bisects the nuclear compartment. An example of a microvascular endothelial cell and pericyte with FOXO1 nuclear translocation is evident in Fig. 1. Microvascular cells that were positive for FOXO1 nuclear translocation typically exhibited increased cytoplasmic expression consistent with an overall increase in expression. Conversely, cells without FOXO1 nuclear translocation typically exhibited only faint FOXO1 immunofluorescence in the cytoplasm, indicating a low basal level of expression as indicated (Fig. 1). Additional images demonstrating the FOXO1 nuclear staining in microvascular cells are shown in the online appendix (online appendix Figs. 1–3 [available at <http://dx.doi.org/10.2337/db08-0537>]). The number of retinal microvascular cells with FOXO1 in the nuclear compartment increased fivefold in type 1 diabetic rats that had been hyperglycemic for ~ 6 months (Fig. 1C) and almost fourfold in type 2 diabetic rats (Fig. 1D) compared with normoglycemic rats. The midretinal area was further examined and cells that were positive for FOXO1 nuclear staining based upon the confocal microscopic images were characterized as endothelial cells, pericytes, or undetermined based upon the shape and location of nuclei (as described in 16). FOXO1 nuclear translocation-positive microvascular cells were primarily endothelial cells with an endothelial cell to pericyte ratio of $\sim 2:1$ (Table 1).

To investigate a potential mechanism for diabetes-enhanced FOXO1 nuclear translocation, rats were treated with pegsunercept. TNF inhibition for 12 weeks reduced cells with FOXO1-positive nuclei by 76% in type 1 diabetic (Fig. 1C) and 65% in type 2 diabetic (Fig. 1D) rats. Diabetes increased FOXO1 mRNA more than twofold (Fig. 1E), and pegsunercept reduced it by 64% ($P < 0.05$) (Fig. 1E). Similarly type 1 diabetes increased FOXO1 DNA binding activity more than twofold (Fig. 1F), and TNF inhibition reduced this increase by 74% ($P < 0.05$) in the STZ-induced diabetic rats (Fig. 1F). Diabetes also significantly increased FOXO1 DNA binding in retinas of type 2 diabetic rats (Fig. 1G).

FOXO1 inhibition by RNAi reduces microvascular cell apoptosis in diabetic retinas in vivo. A single intravitreal injection of FOXO1 siRNA 10 days before the rats were killed blocked virtually all of the diabetes-increased FOXO1 mRNA, demonstrating efficacy of RNAi in vivo ($P < 0.05$) (Fig. 2A). Scrambled siRNA had no effect

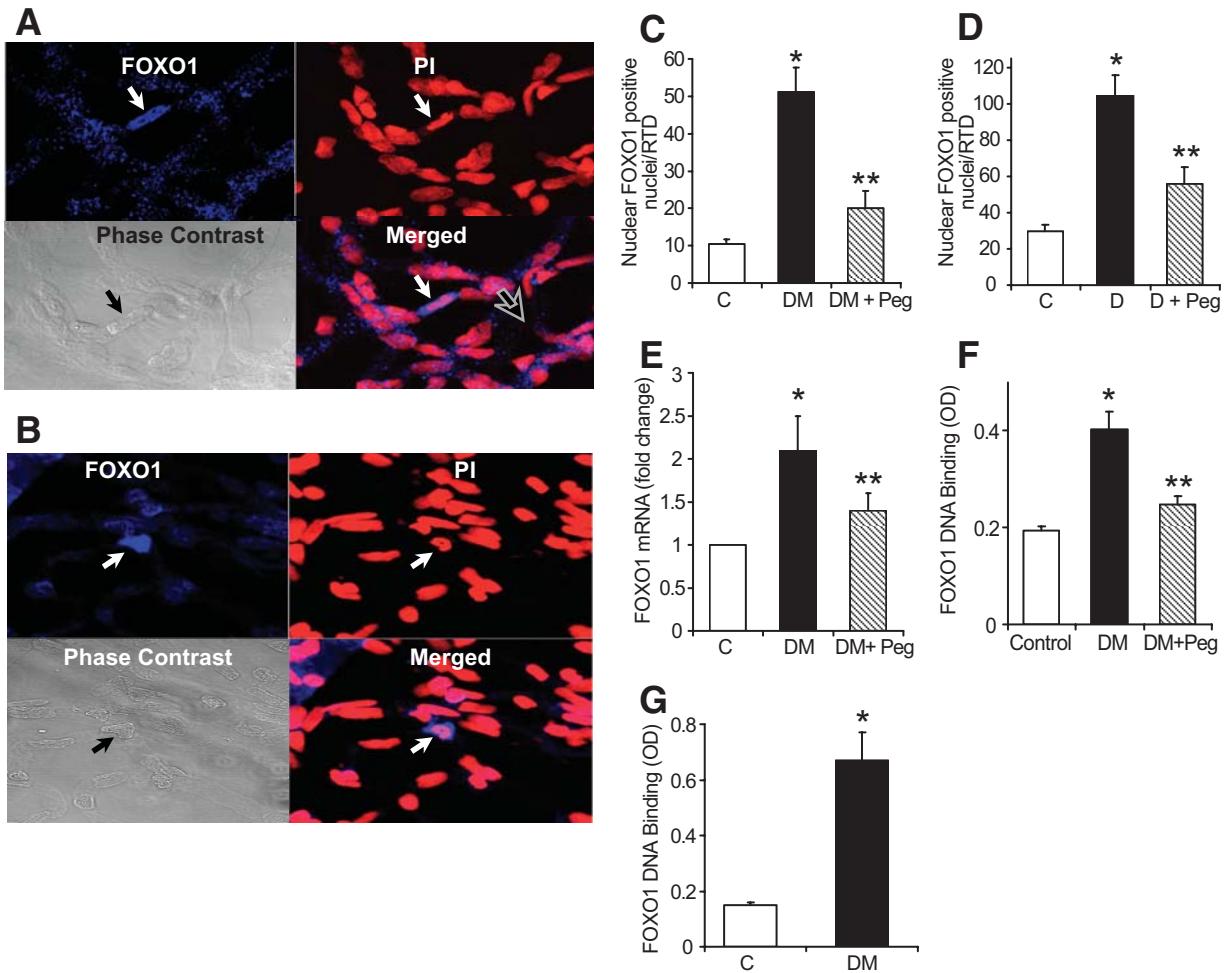


FIG. 1. Diabetes-induced increase in FOXO1 mRNA, DNA binding, and nuclear translocation in the retina is partly dependent on TNF- α . **A:** RTDs from diabetic rats that were hyperglycemic for ~6 months along with age-matched normoglycemic rats were incubated with antibody to FOXO1 and Cy5-tagged secondary antibody (upper left), counterstained with propidium iodide (upper right), and examined by confocal laser-scanning microscopy. Merged FOXO1/propidium iodide (lower right) and phase-contrast (lower left) images are shown. Arrow points to nuclear FOXO1-positive endothelial cells. Incubation with control antibody revealed no staining (data not shown). Original magnification $\times 400$. **B:** RTDs from diabetic rats that were hyperglycemic for ~6 months along with age-matched normoglycemic rats were incubated with antibody to FOXO1 and Cy5-tagged secondary antibody (upper left), counterstained with propidium iodide (upper right), and examined by confocal laser-scanning microscopy. Merged FOXO1/propidium iodide (lower right) and phase-contrast (lower left) images are shown. Arrow points to nuclear FOXO1-positive pericytes. Incubation with control antibody revealed no staining (data not shown). Original magnification $\times 400$. **C:** The mean number of cells with clearly identified FOXO1 nuclear translocation was determined in STZ-induced diabetic rats (DM), STZ-induced diabetic rats treated with pegsunercept (DM + Peg), and age-matched normoglycemic control (C) rats. Each value is the mean \pm SE ($n = 5$ /group). **D:** The mean number of cells with clearly identified FOXO1 nuclear translocation was determined in ZDF rats treated with vehicle alone (D), ZDF rats treated with pegsunercept (D + Peg), and age-matched normoglycemic control (C) rats. Each value is the mean \pm SE ($n = 6$ /group). **E:** RNA was isolated from whole retinas and mRNA levels of FOXO1 determined by real-time PCR from STZ-induced diabetic rats (DM) that had been hyperglycemic for 12 weeks and treated with vehicle alone, diabetic rats treated with pegsunercept (DM + Peg) for 8 weeks before euthanasia, and age-matched normoglycemic control (C) rats. The data presented is mean fold change \pm SE ($n = 6$ /group). **F:** Nuclear proteins were isolated from whole retina of STZ-induced diabetic rats (DM) with hyperglycemia of 12 weeks duration treated with vehicle alone, STZ-induced diabetic rats treated with pegsunercept (DM + Peg) for 8 weeks before euthanasia, and age-matched normoglycemic control (C) rats. Nuclear proteins were assayed for FOXO1 DNA binding activity using a transcription factor ELISA. Each value is the mean \pm SE ($n = 6$ /group). **G:** Nuclear proteins were isolated from whole retinas of ZDF rats (DM) with 12 weeks hyperglycemia and age-matched normoglycemic control (C) rats. Nuclear proteins were assayed for FOXO1 DNA binding activity. Each value is the mean \pm SE ($n = 6$ /group). *Significantly higher in the diabetic than normoglycemic group ($P < 0.05$). **Significantly less in pegsunercept than vehicle-treated rats ($P < 0.05$). (Please see <http://dx.doi.org/10.2337/db08-0537> for a high-quality digital representation of this figure.)

TABLE 1
Distribution of cells with FOXO1 nuclear translocation in RTDs

	Distribution of cells with FOXO1 nuclear translocation (%)
Endothelial cells	63
Pericytes	28
Undetermined	9

Data are percent. Midretinal areas in RTDs were scored, and cells with FOXO1 nuclear localization were assessed in confocal laser-scanning microscopic images. Cells were categorized as endothelial cells, pericytes, or undetermined based on the shape and location of nuclei as described in RESEARCH DESIGN AND METHODS.

($P > 0.05$). In long-term experiments, FOXO1 siRNA applied 6 and 12 weeks before the type 1 diabetic rats were killed reduced diabetes-enhanced FOXO1 nuclear translocation in microvascular cells by 86% ($P < 0.05$) (Fig. 2B). Scrambled siRNA had no effect ($P > 0.05$).

The role of FOXO1 in microvascular apoptosis and the cumulative effect of apoptosis as reflected by pericyte ghost formation and the development of acellular capillaries was examined (23). Type 1 diabetes increased the number of TUNEL-positive cells sevenfold, which was reduced 75% by FOXO1 siRNA ($P < 0.05$) in the STZ-induced diabetic rats (Fig. 2C). Diabetes induced a sixfold increase in pericyte ghost formation, which was reduced

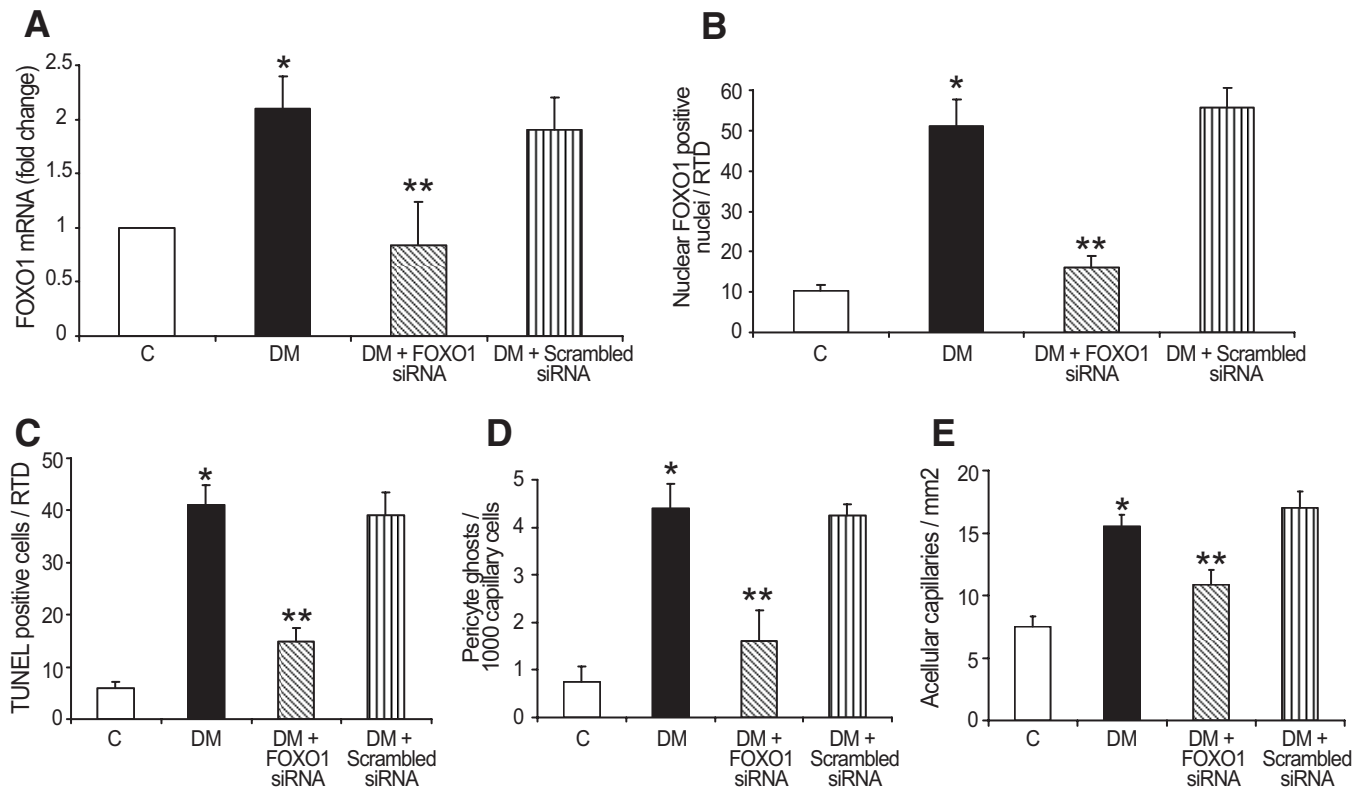


FIG. 2. FOXO1 siRNA effectively reduces FOXO1 mRNA level and nuclear translocation in vivo and reduces diabetes induced microvascular cell loss in STZ-induced diabetic rats. **A:** RNA was isolated from whole retinas and mRNA levels of FOXO1 determined by real-time PCR from STZ-induced diabetic rats (DM) that had been hyperglycemic for 12 weeks, matched diabetic rats treated with FOXO1 siRNA (DM + FOXO1 siRNA) or scrambled siRNA (DM + scrambled siRNA) for 10 days before euthanasia, and age-matched normoglycemic control (C) rats. Data represent mean relative fold change compared with control \pm SE ($n = 5/\text{group}$). **B:** The mean number of cells with clearly identified FOXO1 nuclear translocation in STZ-induced diabetic rats (DM) that had been hyperglycemic for ~ 6 months, matched diabetic rats treated with FOXO1 siRNA (DM + FOXO1 siRNA), scrambled siRNA (DM + scrambled siRNA) applied by two intravitreal injections at 12 and 6 weeks before euthanasia, and age-matched normoglycemic control (C) rats ($n = 5/\text{group}$). Data represent the mean \pm SE. **C:** The mean number of TUNEL-positive microvascular cells was determined in STZ-induced diabetic rats (DM) that had been diabetic for ~ 6 months, matched diabetic rats treated with FOXO1 siRNA (DM + FOXO1 siRNA), or scrambled siRNA (DM + scrambled siRNA) and age-matched normoglycemic control (C) rats, by intravitreal injections at 12 and 6 weeks before euthanasia ($n = 5$). **D:** The mean number of pericyte ghosts was determined in PAS-stained RTDs from groups described above in (C). **E:** The mean number of acellular capillaries was determined in PAS-stained RTDs from groups described above in (C). Data represent the means \pm SE. *Significantly higher in diabetic than normoglycemic rats ($P < 0.05$). **Significantly less with FOXO1 siRNA compared with scrambled siRNA ($P < 0.05$).

$\sim 75\%$ by FOXO1 siRNA ($P < 0.05$) (Fig. 2D and supplemental Fig. 6). Similarly, type 1 diabetes increased acellular capillary formation by twofold ($P < 0.05$), and FOXO1 siRNA reduced this increase by $\sim 60\%$ ($P < 0.05$) in the STZ-induced diabetic rats (Fig. 2E). For all three parameters, scrambled siRNA had no effect ($P > 0.05$).

FOXO1 RNAi reduces microvascular cell apoptosis in the retina of type 2 diabetic rats. The impact of silencing FOXO1 on microvascular cell apoptosis was assessed in retinal trypsin digests in type 2 diabetic animals. An 8-fold increase in retinal microvascular endothelial cells expressing activated caspase-3 caused by diabetes was reduced 74% by FOXO1 siRNA ($P < 0.05$) (Fig. 3A), and a 10-fold increase in pericytes was reduced by 80% ($P < 0.05$) (Fig. 3A). FOXO1 siRNA also reduced the fivefold increase in diabetes-enhanced TUNEL-positive endothelial cells by 79% and the fivefold increase in TUNEL-positive pericytes by 71% ($P < 0.05$) (Fig. 3B). Scrambled siRNA had no effect ($P > 0.05$). Representative images of caspase-3 and TUNEL-positive retinal microvascular endothelial cells are shown in supplemental Figs. 4 and 5. As an additional control, immunohistochemistry experiments were carried out with antibody to CD18, demonstrating that there were very few immune cells trapped within the microvasculature and none of these

were apoptotic when immunohistochemistry with CD18 was combined with the TUNEL assay (data not shown).

High glucose stimulates FOXO1 DNA binding and modulates FOXO1 phosphorylation in RMECs in vitro, and high-glucose-stimulated apoptosis is reduced by FOXO1 silencing. Incubation of RMECs with high glucose induced a dose-dependent increase in FOXO1 DNA binding that was increased 2.3-fold in 25 mmol/l glucose compared with standard glucose (5 mmol/l), while D-mannitol (25 mmol/l) had no effect ($P > 0.05$) (Fig. 4A), demonstrating that the effect is not due to osmotic shock. To establish whether high glucose altered FOXO1 protein and its phosphorylation status, assays were performed in cellulo. High glucose significantly increased total FOXO1 protein level twofold, while simultaneously reducing phosphorylated FOXO1 by 37% ($P < 0.05$) (Fig. 4B), consistent with FOXO1 activation. High glucose increased FOXO1 mRNA level 1.7-fold ($P < 0.05$), and transfection with FOXO1 siRNA reduced it by 61% ($P < 0.05$) (Fig. 4C). FOXO1 siRNA also reduced total FOXO1 protein levels in high-glucose-stimulated RMECs by 57% compared with scrambled siRNA ($P < 0.05$) (Fig. 4D), consistent with reports that siRNA achieves knockdown for 5 days in dividing cells and 3 weeks in nondividing cells (24). High glucose induced a 2.3-fold increase in RMEC apoptosis,

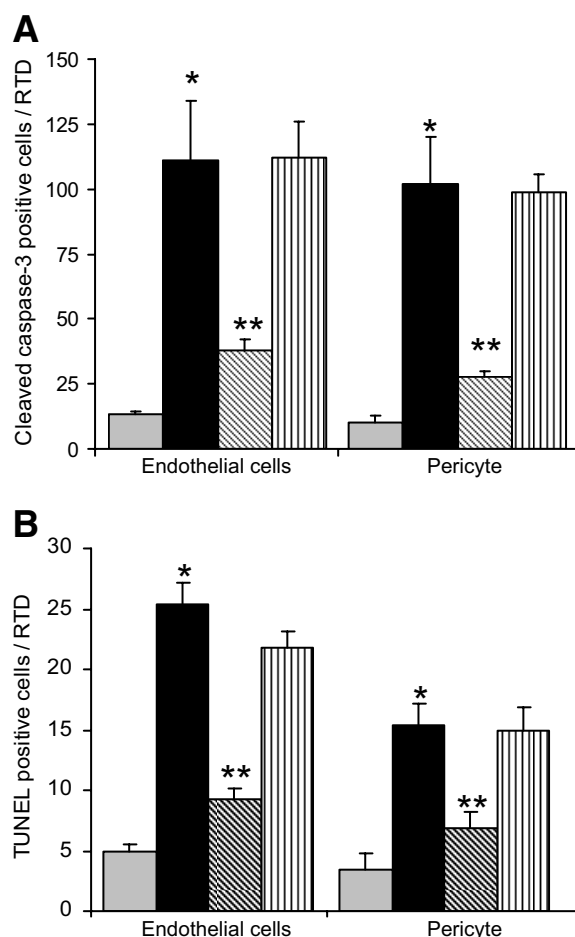


FIG. 3. FOXO1 siRNA reduces retinal microvascular endothelial cell and pericyte apoptosis in ZDF rats. **A:** The mean number of cleaved caspase-3-positive endothelial cells and pericytes were determined in RTDs from ZDF rats that were hyperglycemic for ~6 months (DM, ■), ZDF rats treated with FOXO1 siRNA (DM + FOXO1 siRNA, ▨), ZDF rats treated with scrambled siRNA (DM + scrambled siRNA, □), and from age-matched normoglycemic control rats (C, ▤), applied by an intravitreal injection 10 days before euthanasia. Pericytes and endothelial cells were determined by comparison of a bright field image of the same field PAS stained. **B:** The mean number of TUNEL-positive endothelial cells and pericytes were measured in RTDs from ZDF rats that were hyperglycemic for ~6 months (DM), ZDF rats treated with FOXO1 siRNA (DM + FOXO1 siRNA), ZDF rats treated with scrambled siRNA (DM + scrambled siRNA), and from age-matched normoglycemic control (C) rats, as described in B. Each value represents the mean number per RTD \pm SE. ($n = 6$ /group). *Significantly higher in diabetic than normoglycemic rats ($P < 0.05$). **Significantly less with FOXO1 siRNA compared with scrambled siRNA ($P < 0.05$).

and FOXO1 siRNA transfection resulted in 70% reduction in high-glucose-stimulated apoptosis ($P < 0.05$) (Fig. 4E). **High glucose reduces phosphorylated AKT and FOXO1 levels in RMECs in vitro.** Incubation in high glucose caused a 32% reduction ($P < 0.05$) in phosphorylated Akt without affecting AKT protein levels (Fig. 5A). The functional importance of Akt in FOXO1 was assessed by using an Akt inhibitor, which further reduced high-glucose-diminished FOXO1 phosphorylation by 52% compared with high glucose alone ($P < 0.05$) (Fig. 5B). The Akt inhibitor did not affect FOXO1 protein levels (Fig. 5C).

TNF inhibition reduces high-glucose-induced FOXO1 DNA binding activity and high-glucose-induced FOXO1 DNA binding in a reactive oxygen species-dependent manner. Both high glucose and TNF stimulate FOXO1 DNA binding activity (Fig. 5D and E). Moreover, TNF, in part, mediates high-glucose-stimulated FOXO1 DNA bind-

ing since pegsunercept reduces it by >42% ($P < 0.05$) (Fig. 5D). FOXO1 siRNA also reduced FOXO1 mRNA levels by 65% in RMECs stimulated with TNF- α ($P < 0.05$) compared with scrambled siRNA (Fig. 5E) and reduced TNF- α -stimulated apoptosis of RMECs by 64% ($P < 0.05$) (Fig. 5F). To identify the potential upstream and downstream mechanism, in vitro experiments with RMECs revealed that high-glucose-induced FOXO1 DNA binding returned to baseline levels when reactive oxygen species (ROS) inhibitor was used compared with high glucose alone (Fig. 5G). Under similar conditions, apoptosis was reduced by >61% when ROS formation was inhibited (Fig. 5H). High glucose also led to greater caspase-3/7 activation, and FOXO1 siRNA reduced high-glucose-induced caspase-3/7 activation by >50% ($P < 0.05$) (Fig. 5I). In addition, when a caspase-3/7 inhibitor was used, high-glucose-stimulated apoptosis was reduced by 50% ($P < 0.05$) (Fig. 5J). Thus, high glucose appears to induce RMECs apoptosis through a mechanism that involves reduced FOXO1 phosphorylation and increased FOXO1 mRNA, protein, and DNA binding activity. Furthermore, high-glucose-induced FOXO1 DNA binding activity or apoptosis is mediated by formation of ROS and TNF.

FOXO1 regulates high-glucose-induced gene expression. To identify potential mechanisms through which FOXO1 may mediate the effects of hyperglycemia, mRNA profiling with focused microarrays was undertaken. The mean and median values of three microarrays per assay conditions are shown compared with the mean on the corresponding control with a threshold set at a minimum 1.7-fold increase or 0.58-fold decrease. The genes were divided into three functional groups regulating endothelial cell activation, endothelial cell apoptosis, and angiogenesis (Table 2). High glucose enhanced the mRNA levels of 10 of 14 genes (CCL2, CCL5, F3, ICAM1, IL6, PLAT, TFPI, TFPI2, THBD, and VCAM1) that modulate endothelial cell activation by 2.0- to 3.5-fold. FOXO1 siRNA reduced mRNA levels of all 14 genes belonging to this group by 0.12- to 0.58-fold. All eight genes (BCL2, CASP3, CASP6, TNF- α , TNFRSF11B, BCL2A1, BIRC3, and BIRC4) tested that are involved in apoptosis were increased by high glucose from 1.7- to 2.9-fold. FOXO1 siRNA reduced mRNA levels of five (BCL2, CASP3, CASP6, TNF- α , and TNFRSF11B) of these from 0.34- to 0.45-fold.

The majority of genes involved in angiogenesis were not modulated by high glucose but were by FOXO1 (Table 2). High glucose stimulated an increase in mRNA levels of 4 (ITGB1, ANGPT1, FLT4, and VEGF) of 10 of these genes from 2.6- to 4.9-fold. FOXO1 siRNA reduced mRNA of these four as well as others (ITGA5, ITGAV-M, ITGB3, KDR, and TEK) by 0.29- to 0.54-fold. Genes from each functional category were selected and results with microarrays were confirmed by real-time PCR (Fig. 6). For CASP-3, ICAM1, VEGF, and TNF- α , stimulation with high glucose induced a minimum 1.7-fold increase and inhibition by FOXO1-induced a 0.58-fold decrease whether assayed by microarray or by real-time PCR.

DISCUSSION

We report for the first time that diabetes increases FOXO1 mRNA levels and DNA binding activity in the retina. In addition, both type 1 and type 2 diabetic models exhibited increased FOXO1 nuclear translocation in retinal microvascular cells. These increases occurred in a time frame when increased inflammation, caspase-3-positive cells,

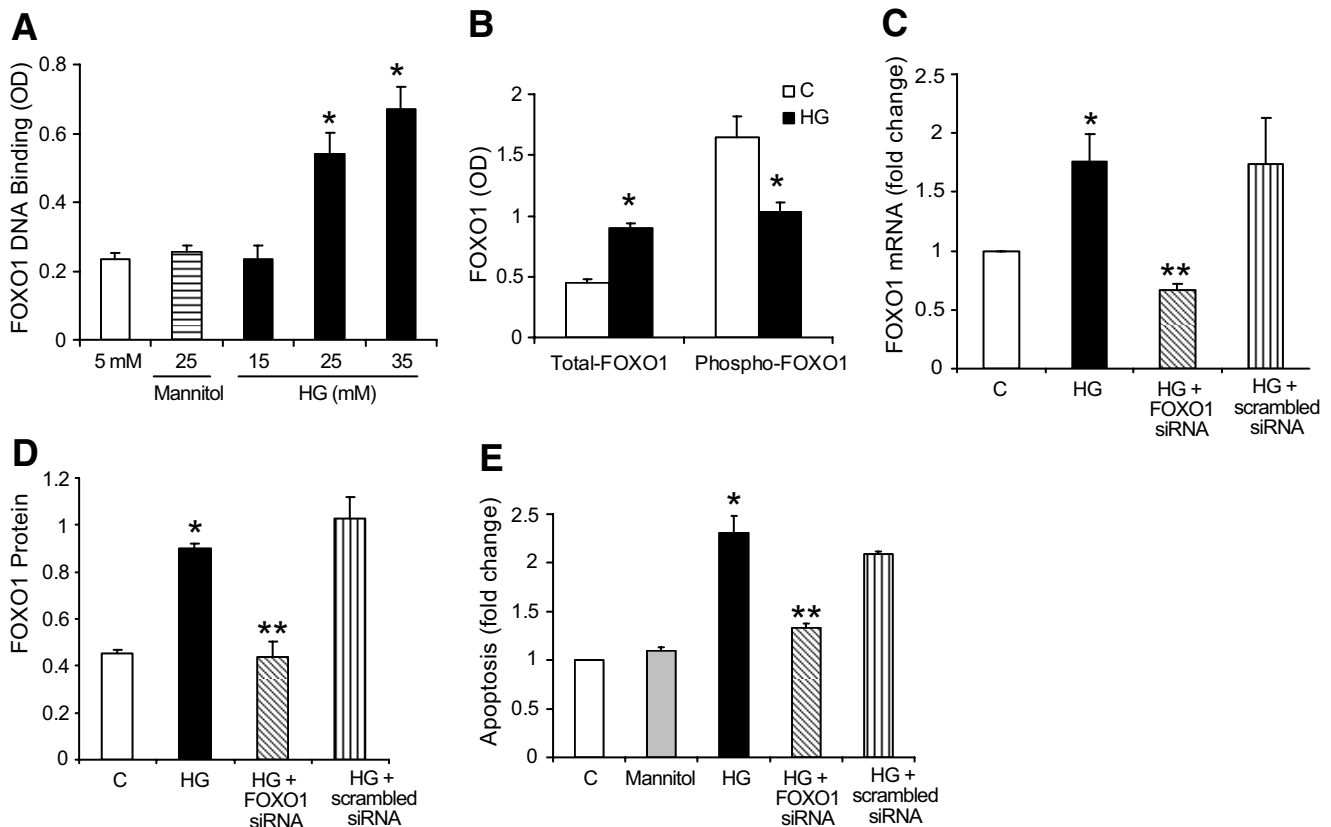


FIG. 4. High glucose enhances FOXO1 DNA binding and decreases FOXO1 phosphorylation in the retinal microvascular endothelial cells in vitro, and FOXO1 siRNA reduces high glucose increased FOXO1 mRNA, protein, and apoptosis. **A:** RMECs were incubated in standard culture media (5 mmol/l glucose), media with high glucose (15–35 mmol/l), or media with 25 mmol/l mannitol for 5 days. Extracted nuclear proteins were tested for FOXO1 DNA binding activity by transcription factor ELISA. **B:** RMECs were incubated with standard media (C) or high-glucose media, 25 mmol/l (HG). Following treatment, total and phosphorylated FOXO1 levels were measured in cellulo. **C:** RMECs were transfected with FOXO1 siRNA or scrambled siRNA in vitro for 24 h. After transfection cells were incubated in standard media (5 mmol/l) or media with high glucose (25 mmol/l) for 5 days. mRNA levels of FOXO1 were determined by real-time PCR and normalized by the level of 18S rRNA in the same sample. **D:** cells treated as in **C** were assessed for FOXO1 protein in cellulo. **E:** Cells described in **C** were assayed for apoptosis by ELISA measuring cytoplasmic histone-associated DNA. Each value represents the mean \pm SE obtained from three independent experiments.

and enhanced apoptosis are present (8–26 weeks). Moreover, TNF-mediated diabetes enhanced FOXO1 mRNA levels, DNA binding, and nuclear translocation. Thus, we propose that diabetes increases TNF- α , which enhances FOXO1 mRNA levels, nuclear translocation, and DNA binding in retinas of type 1 and type 2 diabetic rats.

The functional significance of FOXO1 was tested by RNAi. Intravitreal injection of FOXO1 siRNA significantly reduced FOXO1 mRNA levels and FOXO1 nuclear translocation, while control-scrambled siRNA had no effect. The effect of FOXO1 knockdown by siRNA was evident 6 weeks after the second injection, indicating that silencing is effective for at least 6 weeks. In type 1 diabetic rats, FOXO1 siRNA significantly decreased microvascular cell apoptosis, the formation of pericyte ghosts, and the development of acellular capillaries. Similar results were found in type 2 diabetic rats. FOXO1 siRNA significantly reduced cleaved caspase-3- and TUNEL-positive pericytes and endothelial cells. This represents the first demonstration that FOXO1 plays a critical role in diabetes-induced apoptosis and retinal microvascular cell loss.

In retinal microvascular endothelial cells, high glucose was shown to increase FOXO1 mRNA and protein levels. In addition, high glucose reduced FOXO1 phosphorylation, consistent with increased DNA binding activity, since FOXO1 is deactivated by phosphorylation. High glucose did not affect total Akt levels but did significantly decrease the active phosphorylated isoforms of Akt. When Akt was

inhibited there was a further decrease in FOXO1 phosphorylation, indicating that high glucose levels could modulate FOXO1 through its effect on Akt. In addition, hypoinsulinemia or insulin resistance associated with diabetes could potentially contribute to decreased phosphorylation of Akt in vivo and contribute to enhanced FOXO1 activity (25).

As discussed above, TNF-mediated diabetes enhanced FOXO1 activation both in vitro and in vivo. Furthermore, TNF stimulated apoptosis that was reduced by FOXO1 siRNA. Similarly, ROS inhibitor reduced high-glucose-stimulated FOXO1 DNA binding activity and high-glucose-induced apoptosis. Also, high-glucose-stimulated apoptosis was inhibited by FOXO1 siRNA. Thus, several pathways by which high glucose increased FOXO1 were tested. In each case, the factor was shown to mediate high-glucose-stimulated apoptosis of retinal endothelial cells. The results obtained in vitro and in vivo are strikingly similar and indicate that hyperglycemia per se could stimulate apoptosis of microvascular cells through a mechanism not involving other cell types, although it cannot be ruled out that other cell types or leukostasis in the retina may play an important role in the apoptotic process (26,27).

In vitro mRNA profiling suggests that FOXO1 mediates high-glucose-induced mRNA expression of genes that modulate endothelial cell activation and apoptosis and the basal expression of genes that affect angiogenesis, which

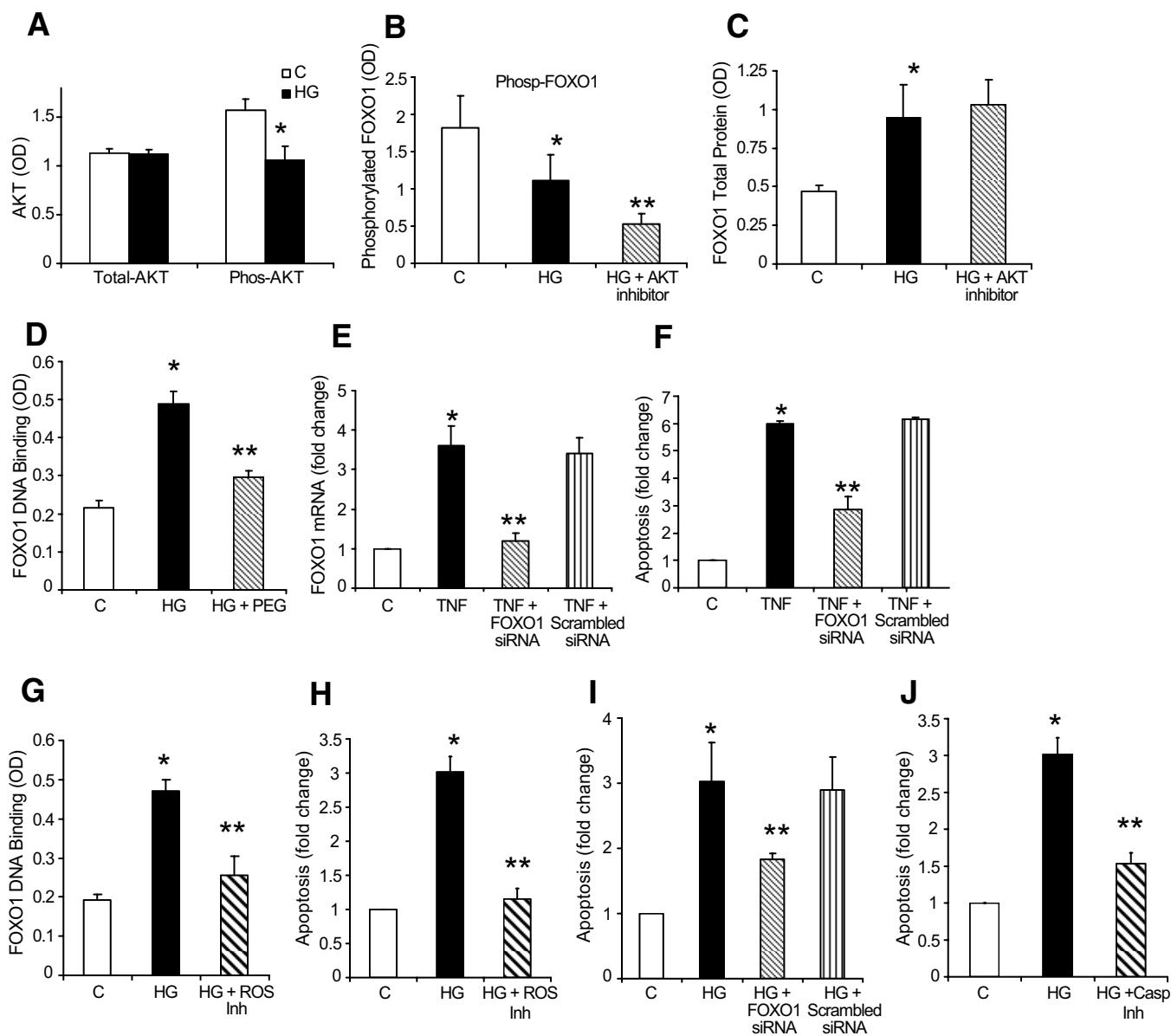


FIG. 5. High glucose modulates AKT and FOXO1 and high glucose induced apoptosis is mediated by TNF, ROS, FOXO1, and caspase-3 in retinal microvascular endothelial cells. **A:** RMECs were incubated with standard media (C) or high glucose (HG) for 5 days as described above and assayed for AKT protein and phosphorylated AKT in cellulo. **B:** RMECs were incubated with standard media (C; 5 mmol/l), high glucose (HG; 25 mmol/l), or high glucose with AKT inhibitor (HG + AKT inhibitor) for 5 days and assayed for phosphorylated FOXO1 protein. **C:** RMECs were incubated with standard media (C; 5 mmol/l), high glucose (HG; 25 mmol/l), or high glucose with AKT inhibitor (HG + AKT inhibitor) for 5 days and assayed for total FOXO1 protein. **D:** RMECs were incubated with standard media (C), high-glucose media, 25 mmol/l (HG), and high-glucose media plus 10 μ g/ml pegsunercept (HG + Peg) for 5 days. Following treatment, extracted nuclear proteins were tested for FOXO1 DNA binding by transcription factor ELISA. **E:** RMECs were transfected with FOXO1 siRNA or scrambled siRNA as described in **A** and incubated with or without TNF- α (20 ng/ml) for 6 h. mRNA levels of FOXO1 were determined by real-time PCR and normalized by the level of 18S rRNA in the same sample. **F:** RMECs were transfected with FOXO1 siRNA or scrambled siRNA followed by stimulation with or without TNF- α (20 ng/ml) for 6 h. Apoptosis was determined by ELISA measuring histone-associated cytoplasmic DNA. **G:** RMECs were incubated with standard media (C; 5 mmol/l); high glucose (HG; 25 mmol/l); high glucose with NAC, a ROS inhibitor (10 mmol/l) (HG + NAC); and nuclear proteins were extracted and tested for FOXO1 DNA binding activity. **H:** Cells were incubated in standard media (C), high-glucose media (HG), or high glucose plus NAC (10 mmol/l) (HG + ROS Inh). **I:** RMECs were transfected with FOXO1 siRNA or scrambled siRNA in vitro for 24 h. After transfection cells were incubated in standard media (5 mmol/l) or media with high glucose (25 mmol/l) for 5 days. Caspase-3/-7 activity was measured using a luminescent substrate. **J:** RMECs were incubated with standard media (C; 5 mmol/l), high glucose (HG; 25 mmol/l), high glucose with caspase-3 inhibitor (10 μ mol/l) (HG + Z-DEVD-FMK) for 5 days and assayed for apoptosis as described in **F**. Each value represents the mean of three independent experiments \pm SE. *Significantly different in high glucose compared with standard glucose ($P < 0.05$). **Significantly different in treated high glucose compared with untreated high glucose.

were not altered by high-glucose conditions. A surprising finding was that FOXO1 siRNA reduced mRNA levels of several genes that regulate proinflammatory and procoagulant responses. Thus, FOXO1 could induce expression of genes that participate in the very early events that affect diabetic retinal microvascular endothelial cells, many of which are known to be increased by diabetes (28–30). This

is significant since it has not previously been recognized that FOXO1 could modulate proinflammatory gene expression. However, it is consistent with activation of FOXO1 during the early inflammatory phase of diabetic retinopathy. In addition, FOXO1 siRNA modulated a high percentage of proapoptotic genes, consistent with its known proapoptotic function (20). This is supported by data

TABLE 2
Genes regulated by high glucose or high glucose plus FOXO1 siRNA in RMECs

Gene	Unique identification	High glucose		High glucose plus FOXO1 siRNA	
		Mean	Median	Mean	Median
Endothelial cell inflammation/activation					
CCL2	Rn.4772	2.2	1.7	0.4	0.3
CCL5	Rn.8019	2.1	2.1	0.1	0.1
CXCL1	Rn.10907	2.8	2.5	0.3	0.2
ICAM1	Rn0.12	2.3	2.0	0.4	0.4
IL6	Rn.9873	2.4	2.0	0.3	0.3
IL7	Rn.12573	2.3	1.7	0.3	0.2
VCAM1	Rn.11267	2.8	2.0	0.3	0.3
ANXA5	Rn.3318	1.6	1.6	0.6	0.6
CCL20	Rn.10722	2.4	1.6	0.3	0.3
PBP2	Rn.12572	1.9	1.2	0.5	0.6
CSF2	Rn.44285	1.4	1.2	0.3	0.2
ICAM2	Rn.138519	3.0	1.1	0.2	0.2
INOS	Rn.10400	1.9	1.3	0.4	0.5
SEL-E	Rn.10359	1.7	1.0	0.4	0.3
SEL-L	Rn.10461	1.8	1.1	0.3	0.3
SEL-P	Rn.10012	2.0	1.2	0.3	0.3
TGFB1	Rn.40136	2.6	1.5	0.3	0.2
TGFB2	Rn.24539	2.3	1.5	0.3	0.2
VWF	Rn.35561	1.7	1.1	0.4	0.3
IL11	Rn.47218	1.4	0.7	0.3	0.5
IL15	Rn.2490	2.0	1.1	0.2	0.2
IL3	Rn.10652	1.0	0.5	0.3	0.6
Endothelial cell apoptosis					
BAX	Rn.10668	2.5	2.0	0.5	0.5
BCL2	Rn.9996	2.5	2.1	0.4	0.4
CASP3	Rn.10562	2.9	2.4	0.5	0.5
CASP6	Rn.88160	4.1	4.2	0.3	0.3
CASP8	Rn.54474	2.0	1.9	0.5	0.5
TNFRSF11B	Rn.9792	1.7	1.7	0.3	0.4
TNFRSF10B	Rn.105558	2.6	1.5	0.3	0.4
BCL2A1	Rn.19770	1.7	1.7	0.7	0.7
BIRC3	Rn.64578	1.8	1.7	0.7	0.7
BIRC4	Rn.91239	2.8	1.7	0.7	0.8
Angiogenesis					
ITGB1	Rn.25733	2.6	2.0	0.3	0.3
ANGPT1	Rn.120272	4.9	4.6	0.4	0.4
FLT4	Rn.81043	3.5	2.7	0.2	0.2
VEGFA	Rn.1923	3.0	2.8	0.4	0.3
ITGA5	Rn.100796	2.8	1.1	0.4	0.4
ITGB3	Rn.17129	2.4	1.4	0.3	0.3
KDR	Rn.88869	1.9	1.1	0.4	0.4
MMP2	Rn.6422	2.5	1.6	0.4	0.4
MMP9	Rn.10209	2.1	1.3	0.3	0.4
TEK	Rn.9159	3.9	1.6	0.3	0.3
COL18A1	Rn.12030	2.2	1.3	0.5	0.5
PLG	Rn.20178	1.7	1.1	0.5	0.6

Data are mean and median of three independent arrays for each time point. Boldface indicates that both the mean and median of the experimental group was 1.7- or 0.58-fold of the corresponding control (high glucose versus low glucose; high glucose plus FOXO1 siRNA versus high glucose plus scrambled siRNA). RMECs were incubated with or without high glucose (25 mmol/l) for 5 days. Some cells were transfected with FOXO1 siRNA or scrambled siRNA for 24 h prior to incubation in high glucose for 5 days. Total RNA was isolated and subjected to focused microarray analysis. The table lists genes differentially regulated by high glucose or FOXO1 siRNA in high-glucose-treated microvascular endothelial cells. High glucose: fold change in mRNA level in high-glucose-treated cells versus standard-glucose-treated cells. High glucose plus FOXO1 siRNA: fold change in mRNA level of each gene in cells transfected with FOXO1 siRNA plus high glucose versus scrambled siRNA plus high glucose.

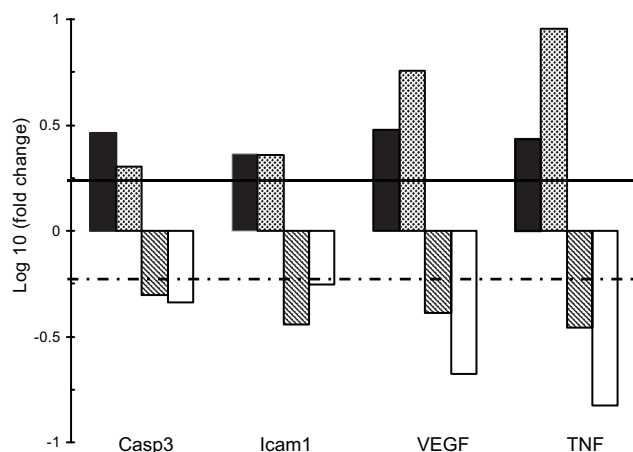


FIG. 6. Comparison of mRNA levels obtained by microarray or real-time PCR. RMECs were transfected with FOXO1 siRNA or scrambled siRNA in vitro for 24 h, transferred to standard media (5 mmol/l) or high-glucose media (25 mmol/l) for 5 days. mRNA levels of CASP3, ICAM1, VEGF-A, and TNF- α were determined by real-time PCR and normalized by the level of 18S rRNA in the same sample. Microarray analysis of the same treatment groups are also shown from values obtained in Table 2. Data presented is the fold change between each experimental group and its control (high glucose compared with standard glucose; FOXO1 siRNA plus HG compared with scrambled siRNA plus HG). The fold change was converted to log₁₀ scale to facilitate comparison between different genes. The horizontal solid line corresponds to 0.23 (log₁₀ equivalent of 1.7 upregulation threshold) and dashed line corresponds to -0.23 (log₁₀ equivalent of 1.7 fold downregulation threshold). ■, microarray high glucose; ▨, microarray HG + FOXO1 siRNA; ▩, quantitative RT-PCR high glucose; □, quantitative RT-PCR HG + FOXO1 siRNA.

reported here that FOXO1 siRNA inhibited high-glucose-stimulated caspase-3 activity and apoptosis in microvascular endothelial cells in vitro. Furthermore, inhibition of caspase-3 blocked high-glucose-stimulated apoptosis, consistent with FOXO1-regulated caspase-3 mRNA levels and caspase-3 activity. Last, mRNA expression of genes associated with angiogenesis were also enhanced by high glucose and/or reduced by FOXO1 siRNA. This is consistent with a report that FOXO1 overexpression induces genes that regulate angiogenesis and vascular remodeling (31). Thus, high glucose and FOXO1 had a dramatic effect on genes that regulate a relatively diverse array of genes that modulate endothelial cell behavior, several of which are thought to contribute to diabetic retinopathy (30). FOXO1 can affect gene expression without directly binding to DNA (32). For example, FOXO1 can regulate transcription by enhancing the activity of CCAAT/enhancer binding protein α or by modulating the DNA binding and transcriptional activity of PAX3 (33,34).

Few studies have examined the role of transcription factors in early diabetic retinopathy, and a limitation of our studies is that it is unknown if these findings pertain to humans with diabetes. Findings from the short-term application of FOXO1 RNAi point to the possibility of using long-term inhibition of FOXO1 by shRNA in diabetic retinopathy. Moreover, FOXO1 may potentially play an important role in other diabetes complications, where locally enhanced inflammation and apoptosis are associated with pathologic changes. In summary, studies presented here demonstrate a mechanistic link between diabetes, enhanced TNF- α levels in the retina, increased FOXO1 nuclear translocation, and microvascular cell apoptosis. This provides a basis for understanding how chronic low-grade inflammation may play a role in early diabetic retinopathy.

ACKNOWLEDGMENTS

This study was supported by National Institutes of Health Grants R01DE17732, R01DE07559, and R01EY014702 and in part by a departmental grant from the Massachusetts Lions Eye Research Organization.

No potential conflicts of interest relevant to this article were reported.

REFERENCES

- Wild S, Roglic G, Green A, Sicree R, King H: Global prevalence of diabetes: estimates for the year 2000 and projections for 2030. *Diabetes Care* 27:1047–1053, 2004
- Fong DS, Aiello L, Gardner TW, King GL, Blankenship G, Cavallerano JD, Ferris FL 3rd, Klein R: Retinopathy in diabetes. *Diabetes Care* 27 (Suppl. 1):S84–S87, 2004
- Mizutani M, Kern TS, Lorenzi M: Accelerated death of retinal microvascular cells in human and experimental diabetic retinopathy. *J Clin Invest* 97:2883–2890, 1996
- Hammes HP: Pericytes and the pathogenesis of diabetic retinopathy. *Horm Metab Res* 37 (Suppl. 1):39–43, 2005
- Benjamin LE: Glucose, VEGF-A, and diabetic complications. *Am J Pathol* 158:1181–1184, 2001
- Kramerov AA, Saghizadeh M, Pan H, Kabosova A, Montenarh M, Ahmed K, Penn JS, Chan CK, Hinton DR, Grant MB, Ljubimov AV: Expression of protein kinase CK2 in astroglial cells of normal and neovascularized retina. *Am J Pathol* 168:1722–1736, 2006
- Yatoh S, Mizutani M, Yokoo T, Kozawa T, Sone H, Toyoshima H, Suzuki S, Shimano H, Kawakami Y, Okuda Y, Yamada N: Antioxidants and an inhibitor of advanced glycation ameliorate death of retinal microvascular cells in diabetic retinopathy. *Diabetes Metab Res Rev* 22:38–45, 2006
- Reiter CE, Wu X, Sandirasegarane L, Nakamura M, Gilbert KA, Singh RS, Fort PE, Antonetti DA, Gardner TW: Diabetes reduces basal retinal insulin receptor signaling: reversal with systemic and local insulin. *Diabetes* 55:1148–1156, 2006
- Accili D, Arden KC: FoxOs at the crossroads of cellular metabolism, differentiation, and transformation. *Cell* 117:421–426, 2004
- Furukawa-Hibi Y, Kobayashi Y, Chen C, Motoyama N: FOXO transcription factors in cell-cycle regulation and the response to oxidative stress. *Antioxid Redox Signal* 5-6:752–760, 2005
- Burgering BM, Kops GJ: Cell cycle and death control: long live Forkheads. *Trends Biochem Sci* 27:352–360, 2002
- Matsumoto M, Han S, Kitamura T, Accili D: Dual role of transcription factor FoxO1 in controlling hepatic insulin sensitivity and lipid metabolism. *J Clin Invest* 116:2464–2472, 2006
- Potente M, Urbich C, Sasaki K, Hofmann WK, Heeschen C, Aicher A, Kollipara R, DePinho RA, Zeiher AM, Dimmeler S: Involvement of Foxo transcription factors in angiogenesis and postnatal neovascularization. *J Clin Invest* 115:2382–2392, 2005
- Stitt TN, Drujan D, Clarke BA, Panaro F, Timofeyeva Y, Kline WO, Gonzalez M, Yancopoulos GD, Glass DJ: The IGF-1/PI3K/Akt pathway prevents expression of muscle atrophy-induced ubiquitin ligases by inhibiting FOXO transcription factors. *Mol Cell* 14:395–403, 2004
- Nakae J, Kitamura T, Kitamura Y, Biggs Wr, Arden K, Accili D: The forkhead transcription factor Foxo1 regulates adipocyte differentiation. *Dev Cell* 4:119–129, 2003
- Behl Y, Krothapalli P, Desta T, DiPiazza A, Roy S, Graves DT: Diabetes-enhanced tumor necrosis factor- α production promotes apoptosis and the loss of retinal microvascular cells in type 1 and type 2 models of diabetic retinopathy. *Am J Pathol* 172:1411–1418, 2008
- Oshitari T, Polewski P, Chadda M, Li A-F, Sato T, Roy S: Effect of combined antisense oligonucleotides against high-glucose- and diabetes-induced overexpression of extracellular matrix components and increased vascular permeability. *Diabetes* 55:86–92, 2006
- Edwards CK 3rd, Martin SW, Seely J, Kinstler O, Buckel S, Bendele AM, Ellen Cosenza M, Feige U, Kohno T: Design of PEGylated soluble tumor necrosis factor receptor type I (PEG sTNF-RI) for chronic inflammatory diseases. *Adv Drug Deliv Rev* 55:1315–1336, 2003
- Roy S, Roth T: Proliferative effect of high glucose is modulated by antisense oligonucleotides against fibronectin in rat endothelial cells. *Diabetologia* 40:1011–1017, 1997
- Alikhani M, Alikhani Z, Graves DT: FOXO1 functions as a master switch that regulates gene expression necessary for tumor necrosis factor-induced fibroblast apoptosis. *J Biol Chem* 280:12096–12102, 2005
- Alikhani M, Alikhani Z, He H, Liu R, Popek BI, Graves DT: Lipopolysaccharides indirectly stimulate apoptosis and global induction of apoptotic genes in fibroblasts. *J Biol Chem* 278:52901–52908, 2003
- Bartlett DW, Davis ME: Insights into the kinetics of siRNA-mediated gene silencing from live-cell and live-animal bioluminescent imaging. *Nucleic Acid Res* 34:322–333, 2006
- Roy S, Sato T, Paryani G, Kao R: Downregulation of fibronectin overexpression reduces basement membrane thickening and vascular lesions in retinas of galactose-fed rats. *Diabetes* 52:1229–1234, 2003
- Gary DJ, Puri N, Won YY: Polymer-based siRNA delivery: perspectives on the fundamental and phenomenological distinctions from polymer-based DNA delivery. *J Control Release* 121:64–73, 2007
- Holz GG, Chepurny OG: Diabetes outfoxed by GLP-1? *Sci STKE* 2005:pe2, 2005
- Barber AJ, Antonetti DA, Kern TS, Reiter CE, Soans RS, Krady JK, Levison SW, Gardner TW, Bronson SK: The Ins2Akita mouse as a model of early retinal complications in diabetes. *Invest Ophthalmol Vis Sci* 46:2210–2218, 2005
- Kowluru RA, Chan PS: Oxidative stress and diabetic retinopathy. *Exp Diabetes Res* 2007:43603, 2007
- Clark PR, Manes TD, Pober JS, Kluger MS: Increased ICAM-1 expression causes endothelial cell leakiness, cytoskeletal reorganization and junctional alterations. *J Invest Dermatol* 127:762–774, 2007
- Masuzawa K, Goto K, Jesmin S, Maeda S, Miyauchi T, Kaji Y, Oshika T, Hori S: An endothelin type A receptor antagonist reverses upregulated VEGF and ICAM-1 levels in streptozotocin-induced diabetic rat retina. *Curr Eye Res* 31:79–89, 2006
- Lorenzi M, Gerhardinger C: Early cellular and molecular changes induced by diabetes in the retina. *Diabetologia* 44:791–804, 2001
- Daly C, Wong V, Burova E, Wei Y, Zabaski S, Griffiths J, Lai KM, Lin HC, Ioffe E, Yancopoulos GD, Rudge JS: Angiotensin-1 modulates endothelial cell function and gene expression via the transcription factor FKHR (FOXO1). *Genes Dev* 18:1060–1071, 2004
- van der Vos KE, Coffey PJ: FOXO-binding partners: it takes two to tango. *Oncogene* 27:2289–9933, 2008
- Sekine K, Chen YR, Kojima N, Ogata K, Fukamizu A, Miyajima A: FOXO1 links insulin signaling to C/EBP α and regulates gluconeogenesis during liver development. *EMBO J* 26:3607–3615, 2007
- Zhang L, Wang C: Identification of a new class of PAX3-FKHR target promoters: a role of the Pax3 paired box DNA binding domain. *Oncogene* 26:1595–605, 2007